Coarse-graining and renormalisation group methods for the elucidation of the kinetics of complex nucleation and growth processes

Peter V Coveney† and Jonathan AD Wattis‡
†Centre for Computational Science, Department of Chemistry,
University College London, 20 Gordon St, London, WC1H 0AJ, UK.
P.V.Coveney@ucl.ac.uk
Tel 020-7679-4560, Fax 020-7679-7463
‡Theoretical Mechanics, School of Mathematical Sciences,
University of Nottingham, University Park, Nottingham, NG7 2RD, UK.
Jonathan.Wattis@nottingham.ac.uk
Tel 0115-951-3857, Fax 0115-951-3837

22 March, 2005.

Abstract

We review our work on generalisations of the Becker-Döring model of cluster-formation as applied to nucleation theory, polymer growth kinetics, and the formation of supramolecular structures in colloidal chemistry. One valuable tool in analysing mathematical models of these systems has been the coarse-graining approximation which enables macroscopic models for observable quantities to be derived from microscopic ones. This permits assumptions about the detailed molecular mechanisms to be tested, and their influence on the large-scale kinetics of surfactant self-assembly to be elucidated. We also summarise our more recent results on Becker-Döring systems, notably demonstrating that cross-inhibition and autocatalysis can destabilise a uniform solution and lead to a competitive environment in which some species flourish at the expense of others, phenomena relevant in models of the origins of life.
Keywords: nucleation, aggregation, coagulation, kinetics, renormalisation.

1 Introduction

The past thirty years has seen a growing interest in and understanding of nonequilibrium phenomena, particularly the constructive role played by irreversible processes in complex, far-from-equilibrium systems [15, 16, 28, 26]. Within the physical and chemical sciences, the study of such nonlinear systems has been extensive, embracing applications as diverse as fluid dynamics, nonlinear optics, chemical reactions and physiology [20, 23, 25, 24]. In mathematical sciences, we have witnessed the development of many courses and centres dedicated to research on nonlinear dynamics.

Notwithstanding all these developments, one particularly important area of inquiry has been largely overlooked. This is the field of nucleation and growth phenomena, processes which by definition are non-equilibrium and whose nonlinear character is familiar in that most characteristic of features – extended periods of quiescence followed by rapid changes in properties. Such features are well-known in all forms of crystal growth, but they also occur in many other areas, such as polymer and colloid chemistry, gas-phase reactions and so on.

Nucleation and growth processes are traditionally regarded as notoriously complex and difficult to study, experimental results often being deemed irreproducible owing to extremely sensitive dependence on initial conditions. This sensitivity is a reflection of the multiscale nature of the nucleation

process, in which truly microscopic events involving the aggregation and/or fragmentation of small numbers of atoms and molecules dictate the large-scale spatial and temporal evolution of the system.

Many present day experiments performed on systems undergoing nucleation and/or growth are performed at levels of resolution which are orders of magnitude less than those of the fundamental microscopic processes. Our own work in this area has been primarily aimed at bridging the length and timescale gaps between a detailed description of the processes taking place on the underlying molecular level and those observed in experiments. Our approach is based on concepts drawn from the modern theory of nonlinear dynamics and statistical mechanics.

The starting point for our work is the seventy-year-old Becker-Döring model (BD) of first-order phase transitions, revisited in the light of modern theoretical developments. In section 2, we introduce the Becker-Döring model of nucleation, discuss the assumptions underlying it, and describe some of its important properties. Sections 3 and 4 form the main body of the paper; section 3 outlines the ideas behind our coarse-graining technique for obtaining a simpler set of differential equations from the infinite coupled system which comprises the Becker-Döring system. A review of various self-assembling and self-replicating systems to which this technique has been applied follows in section 4. This shows how to obtain a system of equations for the evolution of mesoscopic and macroscopic quantities from a microscopic model and how such mesoscopic and macroscopic models can be used to explain the phenomenon of long induction times. Models of chiral polymerisation and RNA-polymerisation based on the Becker-Döring assumptions are reviewed in section 5. The paper concludes with a summary of the diverse systems to which the Becker-Döring theory may be applied and indicates possible areas in which our approaches may be applied in the future.

2 The Becker-Döring equations for aggregation-fragmentation kinetics

The Becker-Döring equations [4] describe the kinetics of a first order phase transition and are a special case of the Smoluchowski coagulation-fragmentation equations [29, 3]. These more general equations model a process in which clusters divide into two fragments of arbitrary size, and clusters of arbitrary sizes can coalesce. Denoting a cluster or chain of r particles by C_r, the processes modelled are $C_r + C_s \rightleftharpoons C_{r+s}$. In contrast with this Smoluchowski model, the Becker-Döring model assumes that only cluster-monomer interactions occur, that is

$$C_r + C_1 \rightleftharpoons C_{r+1}, \tag{1}$$

with forward a_r ($r = 1, 2, \ldots$) and reverse b_{r+1} (which are zero if (1) is irreversible) rate coefficients. In many systems, cluster-cluster interactions do not occur due to clusters being charged, or having a low concentration or being much less mobile than monomers. We note in passing that the Becker-Döring model is not a fully microscopic model as it describes only the *average* behaviour of a system and nothing about its fluctuations.

We first summarise the important properties of the Becker-Döring system of equations [4] which we use as a basis for our kinetic models of cluster-formation. Any physical, chemical or biological system whose non-equilibrium behaviour may be described in terms of rate processes of the form (1) as well as important generalisations, can be analysed in terms of the Becker-Döring system. A wide range of systems can indeed be so described, including nucleation and growth processes, surfactant self-assembly and polymerisation kinetics, as we shall describe below.

The Becker-Döring system of equations is obtained by taking an average over space of the concentrations of each cluster size, which we define by $c_r(t)$. These quantities evolve according to

$$\frac{\mathrm{d}c_1}{\mathrm{d}t} = q(t) - J_1 - \sum_{r=1}^{\infty} J_r, \tag{2}$$

$$\frac{\mathrm{d}c_r}{\mathrm{d}t} = J_{r-1} - J_r, \tag{3}$$

with fluxes

$$J_r = a_r c_r c_1 - b_{r+1} c_{r+1}, \tag{4}$$

Here, $q(t)$ is the rate at which monomers are introduced into the system; in some scenarios this may be given by a prescribed rate (see for example Wattis [35]) but, more generally, it is either taken to be zero – known as the constant mass formulation (for reasons explained below, see (5)) – or $q(t)$ is such that c_1 is kept at some constant value – the constant monomer concentration formulation. This last formulation applies whenever the pool chemical approximation is valid, that is where the monomer concentration is so large that changes to it do not affect the kinetics of the rest of the system (Gray & Scott [23]).

In reversible systems (that is where $a_r \neq 0$, $b_r \neq 0$), there is a quantity Q_r (actually the r-cluster partition function) defined by $a_r Q_r = b_{r+1} Q_{r+1}$ and $Q_1 = 1$ which generates the equilibrium solution $c_r^{(\mathrm{eq})} = Q_r c_1^r$. It will be helpful to introduce the chemical potential of C_r by $\mu_r(t) = \mu_r^{\ominus} + kT \log c_r(t)$, where T is the Temperature, k is Boltzmann's constant and $\mu_r^{\ominus}$ is the chemical potential in some standard state, chosen such that $\mu_1^{\ominus} = 0$. At equilibrium, we have $\mu_r = r\mu_1$ and thus $\mu_r^{\ominus} = -kT \log Q_r$.

One useful property of the system (2)–(4) is that when $q(t) = 0$, it conserves total density (or mass, defined as ϱ); in general we have

$$\varrho = \sum_{r=1}^{\infty} r c_r, \quad \text{satisfying} \quad \frac{\mathrm{d}\varrho}{\mathrm{d}t} = q(t). \tag{5}$$

Also, the constant monomer system has a Lyapunov function

$$V_{c_1} = \sum_{r=1}^{\infty} c_r \left(\log\left(\frac{c_r}{Q_r c_1^r} \right) - 1 \right), \tag{6}$$

with a modified function pertaining to the constant mass formulation ($V_\varrho = \sum_{r=1}^{\infty} c_r(\log(c_r/Q_r)-1)$). The physical interpretation of this function is that it is the free energy of the system, that is it decreases monotonically along any realisation of the system's kinetics. This is useful for proving convergence to equilibrium.

3 Coarse-graining and renormalisation of the Becker-Döring equations

The idea behind coarse-graining has its origins in the renormalisation method used in statistical physics [1, 11, 41, 42, 43]. The so-called renormalisation group method was developed originally by Kenneth Wilson and others (including Michael Fisher, Leo Kadanoff and Ben Widom) in order to handle the properties of self-similarity and scaling observed in critical phenomena. The central idea is that in the vicinity of a critical point, as correlation functions diverge, matter looks the same on *all* length scales; it is then possible to extract macroscopic properties (including various critical exponents) by indefinite coarse-graining of the properties of a system over the length scales involved. The original concept and associated ideas were applied to systems in thermodynamic equilibrium. In more recent times, the approach has been generalised and extended to treat various non-equilibrium phenomena (for examples, see Goldenfeld [22] or Woodruff [44, 45, 46, 47]). We draw on these ideas in order to determine progressively more coarse-grained mesoscopic and ultimately macroscopic properties of systems described by Becker-Döring kinetics and generalisations thereof.

In our generalised Becker-Döring models of cluster-formation we rescale the aggregation number, there being no spatial variable. This procedure has been developed through a successions of

papers [17, 31, 40, 19] which introduce additional features such as secondary nucleation [31], more general size-dependent rate coefficients [19], and improvements to the accuracy of the method [9]. Comparisons of numerical solutions of the full and reduced systems of equations [9] have shown that the coarse-graining procedure is quantitatively accurate, as well as a powerful method for obtaining both qualitative and quantitative descriptions of a wide range of aggregation-fragmentation phenomena which can be fitted to macroscopic data from experiments. Here we summarise the basic ideas behind the coarse-graining process.

Instead of considering all cluster sizes $r = 1, 2, 3, \ldots$, we shall retain just a subset, say $r = \Lambda_n$ $(n = 1, 2, \ldots)$ where Λ_n takes integer values. For simplicity, let us assume the retained sizes are uniformly spaced and given by $r = 1, 4, 7, 10, \ldots$; then we have $r = \Lambda_n = (n-1)\lambda+1$ with $\lambda = 3$. We will eliminate all concentrations $c_r(t)$ except those that correspond to $r = \Lambda_n$ for some n, and redefine the retained concentrations by $x_n = c_{\Lambda_n}$. This is illustrated in Figure 1.

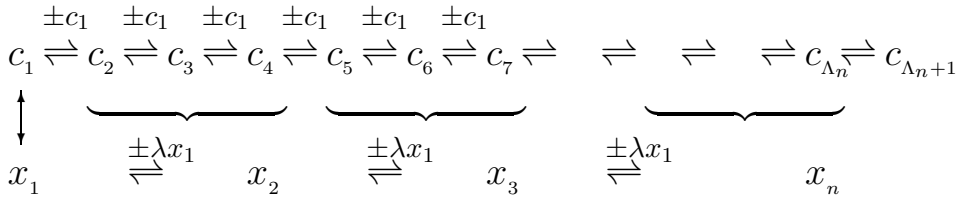

Figure 1: Illustration of the coarse-graining procedure applied to the Becker-Döring equations (1) for the case of a uniform mesh function $\Lambda_n = (n-1)\lambda + 1$ with $\lambda = 3$.

We wish to formulate a system of equations for the concentrations $x_n(t)$ which has a similar structure to the full system (2)–(4); that is, we would like to define quantities analogous to the density and free energy in the reduced system. Hence we postulate

$$\frac{\mathrm{d}x_n}{\mathrm{d}t} = L_{n-1} - L_n, \tag{7}$$

where L_n denotes the flux from size Λ_n with concentration x_n to size Λ_{n+1} and x_{n+1}. The problem is how to define the fluxes L_n in the most appropriate way.

In general, the mesh functions Λ_n need not be uniform; that is, the differences $\lambda_n = \Lambda_{n+1} - \Lambda_n$ may also depend on n. In this more general case, we have

$$\begin{gathered} L_n = \alpha_n x_n x_1^{\lambda_n} - \beta_{n+1} x_{n+1} \\ \alpha_n = T_n a_{\Lambda_n} a_{\Lambda_n+1} \ldots a_{\Lambda_{n+1}-1}, \qquad \beta_{n+1} = T_n b_{\Lambda_n+1} b_{\Lambda_n+2} \ldots b_{\Lambda_{n+1}}. \end{gathered} \tag{8}$$

Our earliest formulations of the procedure omitted the factor T_n. King & Wattis obtained kinetically accurate solutions for the case of size-independent rate coefficients [40] and noted that an additional change of timescale was required. This corresponded to introducing a factor T (with the same value for all sizes n). Thus our coarse-graining procedure can be likened to a dynamical renormalisation process in which time must be rescaled simultaneously with cluster size. In the more detailed study of Bolton & Wattis [9], the form of this size-dependent factor was found for more general size-dependent rate coefficients. In the case of the constant monomer formulation, we have

$$\frac{1}{T_n} = Q_{\Lambda_{n+1}} c_1^{\Lambda_{n+1}} (b_{\Lambda_n+1} b_{\Lambda_n+2} \ldots b_{\Lambda_{n+1}}) \sum_{r=\Lambda_n}^{\Lambda_{n+1}-1} \frac{1}{b_{r+1} Q_{r+1} c_1^{r+1}}. \tag{9}$$

The mass and free energy (Lyapunov function) are then given by

$$\varrho_x = x_1 + \sum_{n=2}^{\infty} \lambda_n \Lambda_n x_n, \qquad V_{x_1} = \sum_{n=1}^{\infty} \lambda_n x_n \left(\log\left(\frac{x_n}{Q_{\Lambda_n} x_1^{\Lambda_n}} \right) - 1 \right). \tag{10}$$

Further information on the theory of the coarse-graining process and applications to systems with general rate coefficients are considered in [19, 36, 37, 9]. We draw attention in particular to the work in [37], where the *stability* of the renormalisation process is examined. There we consider a particular set of rate coefficients ($a_r = ar^p$, $b_{r+1} = br^p$, to be precise) and examine the effect of perturbations to the rate constants on the kinetics of the full system and in the coarse-grained reduction. We find that for $p > 0$ there is little effect, while for $p < 0$ the perturbations dominate at larger cluster sizes. This behaviour is reproduced in the coarse-grained system as well, showing that coarse-graining is a robust method of approximating microscopic models by systems of equations for macroscopic quantities.

4 Application to complex nucleation and growth processes

In this section we discuss a range of complex physicochemical systems and processes which all have an underlying Becker-Döring structure that governs their nonequilibrium behaviour. Several of the systems we have analysed describe the spontaneous self-assembly of surfactant molecules into entities (micelles and vesicles) which can be viewed as proto-cells. Such self-assembly is typically step-wise, that is a structure grows by adsorbing one molecule at a time, the resulting supramolecular entities not interacting directly with one another. Thus the Becker-Döring equations are a suitable framework for modelling the formation such supramolecular structures [14].

4.1 Kinetics of micelle-formation

Our first joint paper [17] applied this approach to interpret the kinetics of self-reproducing micelle-formation in an ethyl caprylate system studied in the experimental work of Bachmann *et al.* [2]. This model system shows the spontaneous formation of cell-like structures (actually ordinary micelles) after a long induction time, and is relevant to origins of life studies. Chemically, the system is composed of an ethyl caprylate precursor (denoted E) which is hydrolysed by aqueous sodium hydroxide to form caprylate monomer (C_1). The monomer aggregates following Becker-Döring kinetics to form micelles with a typical cluster aggregation size of approximately 60. The presence of micelles greatly accelerates the aqueous hydrolysis of ethyl caprylate, thus micelles act as a catalyst for this process. Chemically this can be written as

$$E \xrightarrow{\text{slow}} C_1, \qquad C_r + C_1 \rightleftharpoons C_{r+1}, \qquad E + C_r \xrightarrow{\text{fast}} C_1 + C_r. \tag{11}$$

Thus the overall rate coefficient of the reaction $E \to C_1$ is $\varepsilon + \sum_r k_r c_r$. In (2) this corresponds to $q(t) = e(t)(\varepsilon + \sum_r k_r c_r)$ with $e(t)$ given by

$$\frac{\mathrm{d}e}{\mathrm{d}t} = -e\left(\varepsilon + \sum_{r=2}^{\infty} k_r c_r\right). \tag{12}$$

The effect of this term, together with initial conditions in which all matter is in the form of ethyl caprylate ($e(0) = \varrho$, $c_r(0) = 0$) is that there is a long induction time where ethyl caprylate is broken down slowly, followed by a short phase of rapid kinetics around the critical micelle concentration where micelles start to form accelerating the breakdown of ethyl caprylate. The micelles then rapidly reach their equilibrium distribution. By coarse-graining the combined system of equations (2)–(4) with (12), we were able to construct a simple model involving just three concentrations and described both phases of the reaction with a small number of parameters.

Denoting the monomer concentration by $x(t)$, the rescaled micelle concentration by $y(t)$ and ethyl caprylate by $e(t)$, we derived the following reduced description of the micellisation process

$$\frac{\mathrm{d}e}{\mathrm{d}t} = -\varepsilon e - ye, \quad \frac{\mathrm{d}x}{\mathrm{d}t} = \varepsilon e + ye - \Lambda\alpha x^{\Lambda} - \Lambda\beta y, \quad \frac{\mathrm{d}y}{\mathrm{d}t} = \alpha x^{\Lambda} - \beta x, \tag{13}$$

where $\varrho = e(t)+x(t)+y(t)$ is a conserved quantity (i.e. is constant in time). Centre manifold theory (Carr [12]) or matched asymptotic expansions (Bender & Orszag [7]) then show how the form of the solution arises during the induction time and into the region of rapid kinetics. As well as solving for the initial conditions $e(0) = \varrho$, $x(0) = 0 = y(0)$, we solved the system for $e(0) = \varrho$, $x(0) = \delta$, $y(0) = 0$, to show how a non-zero initial concentration of caprylate anion (δ) reduces the induction time. The model's predictions agree well with experimental results [17].

4.2 Kinetics of self-reproducing vesicle-formation

The system of self-reproducing vesicle formation studied by Walde *et al.* [30] is a logical development of the ethyl caprylate system discussed above. Vesicle-formation is more directly relevant to Luisi's 'autopoiesis' vision of the origin of life via prebiotic cellular compartmentalisation than the micellar system of section 4.1. In order to explain the results of Walde *et al.* [30] we formulated a generalised Becker-Döring model of vesicle-formation [18]. The system is initiated with caprylic anhydride (S) which spontaneously hydrolyses into two caprylic acid molecules at a slow rate. The undissociated acid self-assembles into vesicles which adsorb the anhydride and provide an interface which accelerates the hydrolysis. Thus the model requires two-component clusters denoted $C_{i,n}$ which are composed of a mixture of i hydrolysed surfactant molecules and n anhydride molecules. The microscopic model consists of the reactions

$$\begin{aligned} S &\xrightarrow{\text{slow}} 2C_{1,0}, & C_{i,n} + C_{1,0} &\rightleftharpoons C_{i+1,n}, \\ C_{i,n} + S &\rightleftharpoons C_{i,n+1}, & C_{i,n} &\xrightarrow{\text{fast}} C_{i+1,n-1} + C_{1,0}. \end{aligned} \tag{14}$$

In the last reaction, representing vesicle-catalysed hydrolysis, one molecule is released into the solution and one is adsorbed into the vesicle. Upon applying the coarse-graining reduction to the kinetic equations resulting from (14), we arrive at a system of five equations which describe: (i) the slow spontaneous breakdown of anhydride (S) into caprylic acid monomer (X_1), (ii) the nucleation of small vesicles (X_2 composed of Λ monomers), (iii) growth into large pure vesicles (X_3 of $\Lambda + \lambda$ monomers), (iv) growth into large mixed vesicles (Y which contain Λ monomers and λ anhydride molecules), and (v) the catalytic breakdown of caprylic acid in large mixed vesicles to form a large pure vesicle and anhydride in solution. These processes can be written as

$$\begin{gathered} S \xrightarrow{\text{slow}} 2X_1, \qquad \Lambda X_1 \overset{L_1}{\rightleftharpoons} X_2, \qquad X_2 + \lambda X_1 \overset{L_2}{\rightleftharpoons} X_3, \\ X_2 + \lambda S \overset{L'}{\rightleftharpoons} Y, \qquad Y \xrightarrow{\kappa} X_3 + \lambda X_1, \end{gathered} \tag{15}$$

and are summarised in Figure 2.

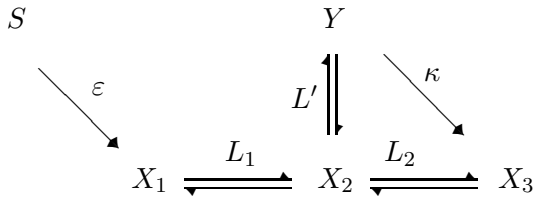

Figure 2: Summary of processes involved in the coarse-grained, macroscopic model of self-reproducing vesicle formation (15).

Further analytic progress in solving the kinetic equations arising from the scheme (15) is made by assuming that the cycle of reactions with fluxes $L_2, L', \kappa y$ are in a local equilibrium, that is $L' = \kappa y = -L_2$. This assumption enables both y and x_3 to be written in terms of x_2, and so

the system can be formulated in terms of just three concentrations, s, x_1, x_2. Conservation of mass simplifies the system further. Matched asymptotic expansions [7] can be used to generate approximate solutions which have the features observed in experiments; see Figure 3. During an initial long timescale, caprylic acid is slowly released to form monomers which assemble into vesicles depending on the latter's concentration. In figure 3 this is shown by the linear rise in total surfactant concentration from $t = 0$ to $t = 17$. Once the critical aggregation concentration is reached the feedback mechanism causes the system to enter a rapid timescale during which the concentration of vesicles increases dramatically (this is not plotted on Figure 3); there then follows a second slow timescale as the system approaches its global equilibrium (shown by the plateauing curve for $t > 18$ in Figure 3).

This experimental and theoretical work has been further extended in the curious size-templating 'matrix' effect observed by Berclaz *et al.* [5, 6] and Blöchliger *et al.* [8]. In these experiments, the size of pre-added vesicles not only accelerates the process of vesicle formation as in the systems discussed above, but also determines the size of vesicles grown from monomers. Bolton and Wattis [10] have proposed a model for this process, which they analysed numerically in the mesoscopic limit and using asymptotic techniques in the macroscopic limit.

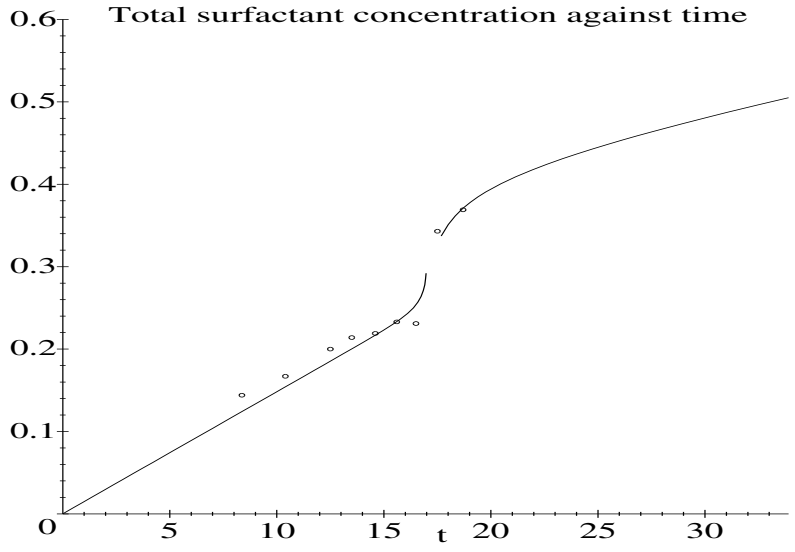

Figure 3: Total surfactant concentration against time for the self-reproducing vesicle experiments and the model (15). During the induction period, this grows linearly, there follows a short period of rapid kinetics, and a slow convergence towards equilibrium. Solid line is prediction based on coarse-grained reduction and solution by matched asymptotic expansions [7], dots represent experimental data from Walde *et al.* [30].

4.3 Nucleation in the presence of an inhibitor

Classical nucleation theory (CNT) typically only aims to model primary, or homogeneous, nucleation. However, in most scenarios secondary, or heterogeneous, nucleation is of at least equal importance. With this nucleation mechanism, the presence of larger crystal nuclei accelerates the formation of smaller nuclei due to small fragments of larger crystals acting as crystal nuclei themselves. This can be modelled by a combination of a Smoluchowski fragmentation term of the form $C_r \to C_k + C_{r-k}$ with rate $b_{k,r-k}$ which would be strongly weighted so that the dominant contribu-

tions come from $k \ll r$ (and, by symmetry, $k = r - \widehat{k}$ with $\widehat{k} \ll r$). Such a mechanism would greatly complicate the model; a simpler, alternative way of modelling the effect is to make the growth rate of smaller nuclei dependent upon the concentration of larger clusters, that is we retain equations (1) but instead of specifying the forward rate by a_r, we let the rate be $a_r + \sum_{s=r}^{\infty} \widehat{a}_{r,s}$.

A further common factor in nucleation processes is the presence of other chemical species which act as inhibitors to growth or nucleation. These effects can be included in a Becker-Döring model by specifying the concentration of an inhibiting species F and including the reaction $F + C_r \to U_r$ where U_r is a poisoned cluster of size r which can undergo no further growth. This increases the complexity of the system, introducing a whole new set of reaction rates and concentrations $u_r(t)$, as well as modifying the equation for c_r. However, such systems are still amenable to reduction by our coarse-graining approach and so an analysis of the macroscopic system is still possible.

In Wattis & Coveney [31] we considered an application of this approach to the complex process of cement hydration, in which the reduced model is

$$P \xrightarrow{k} X_1, \quad \Lambda X_1 \underset{\varepsilon}{\rightleftharpoons} X_2, \quad \Lambda X_1 + \mu X_2 \underset{\alpha}{\rightleftharpoons} (\mu+1)X_2, \quad F + X_2 \xrightarrow{m} V_2, \tag{16}$$

summarised diagramatically in Figure 4. The results from solving this model using matched asymptotic expansions show another type of induction time. We start the system from a state in which there is only precursor (P) and inhibitor (F) present ($x_1(0) = x_2(0) = v_2(0) = 0$). There is an initial equilibration during which monomers are released from the precursor and a balance between monomers and clusters is formed; both being present in small concentrations. A long timescale follows, in which monomers and crystal nuclei remain balanced and at small concentrations; during this timescale nuclei are continually binding to the inhibitor and so effectively being removed from the system. This prevents secondary nucleation accelerating the nucleation kinetics. Finally, when the inhibitor has been exhausted, the concentration of 'healthy' crystal nuclei grows to a level where secondary nucleation accelerates the kinetics and suddenly the system forms a large concentration of non-poisoned crystals.

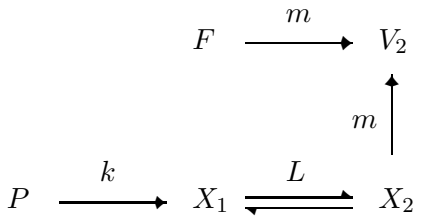

Figure 4: Summary of reduced reaction scheme for nucleation in presence of inhibitor. A precursor (P) decays to form the monomer X_1, which can reversibly aggregate into crystal nuclei X_2 at a rate which, in order to include the effect of secondary nucleation, depends upon the current concentration of crystal nuclei. The system also contains an inhibitor F which can bind to the nuclei forming poisoned clusters V_2.

Our later paper [32] extends the results of this model by analysing the more complex reaction scheme summarised in Figure 5. This model is able to distinguish between the inhibition of nucleation and growth inhibition. All reactions have straightforward kinetics, except for the reversible fluxes L_1 and L_2 which are catalysed by the presence of larger clusters, thus having the forms $L_1 = (x_1^{\Lambda} - \gamma_2 x_2)(\varepsilon\alpha_{10} + \alpha_{12}x_2 + \alpha_{13}x_3)^{\lambda}$ and $L_2 = (x_1^{\mu}x_2 - \gamma_3 x_3)(\varepsilon\alpha_{20} + \alpha_{22}x_2 + \alpha_{23}x_3)^{\mu}$ The results are broadly the same as those described above, with subtle differences depending on the magnitudes of the retained cluster sizes. In one case, for example, growth inhibition occurs at a sufficiently large size that secondary nucleation becomes effective before the inhibitor has been exhausted.

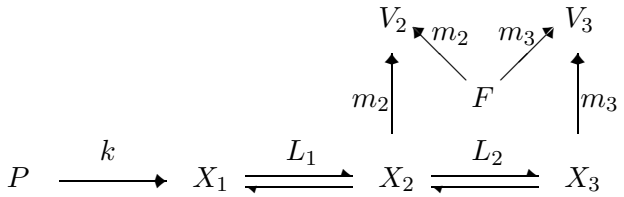

Figure 5: Summary of a less-reduced reaction scheme for nucleation in presence of a secondary species which inhibits nucleation with rate coefficient m_2 and growth with rate coefficient m_3. A precursor (P) decays to form the monomer X_1, which can reversibly nucleate into crystal nuclei X_2 at a rate which, in order to include the effect of secondary nucleation, depends up on the current concentration of larger crystals. These then grow to larger sizes X_3. The system also contains an inhibitor F which can bind to either or both sizes X_2 and X_3 resulting in the formation of poisoned clusters V_2, V_3; note that V_2 cannot grow into V_3.

5 Origins of life

We have already noted that the experimental work led by Luisi [2, 30, 8, 5, 6] is partly motivated by issues arising in origins of life studies. As well as modelling his group's intriguing experimental results as discussed in sections 4.1 and 4.2, we have analysed generalisations of the Becker-Döring model which describe RNA polymerisation and chiral polymerisation. Our two papers [33] and [38] on these systems have recently been the subject of a comparative review [39].

5.1 Origins of homochirality

Many biological macromolecules are chiral yet only one handedness is ever observed in nature. The possible origin of homochirality from a simple achiral chemistry has been modelled by Sandars [27]. We have analysed a similar model [38] and shown that competition for left- and right-handed monomers through enantiomeric cross-inhibition leads to a spontaneous symmetry-breaking, causing the system to be dominated by one or other handedness of molecule.

Our model has both left- and right-handed monomers (denoted L_1 and R_1 respectively) which aggregate into homopolymers (L_n and R_n) via

$$L_n + L_1 \to L_{n+1}, \qquad R_n + R_1 \to R_{n+1}. \tag{17}$$

Enantiomeric cross-inhibition is the process by which the opposite handed monomer can attach to a homopolymer and arrest its further growth:

$$L_n + R_1 \to L_n R_1, \qquad R_n + L_1 \to R_n L_1. \tag{18}$$

To close the model mathematically we assume the existence of some achiral substrate species (S) which can be transformed into either monomer; that is, $S \to L_1$, $S \to R_1$. We also assume the existence of a feedback mechanism with a 'fidelity parameter' f ($0 \le f \le 1$), whereby the existence of homopolymer accelerates the rate of breakdown of S, while an excess of one handedness of homopolymer favours the production of that handedness of monomer. Thus the rate at which L_1 is produced is $\varepsilon + \frac{1}{2}k\sum_n (1+f)nL_n + (1-f)nR_n$, with a similar formula for R_1-production.

Such a system can exhibit solutions in which the two polymer enantiomers grow in equal concentrations. However, the presence of the fidelity parameter and the coupling caused by the enantiomeric cross-inhibition causes such a solution to become unstable for certain ranges of parameter values. For these parameter values, a spontaneous symmetry-breaking occurs, and a solution in which one chirality of polymers dominates the other is observed. We also find that, for stronger enantiomeric cross-inhibition, the bifurcation occurs at smaller values of the fidelity parameter f.

5.2 The origin of the RNA world

One of the principal outstanding questions in origins of life studies is concerned with the origin of the RNA world [21]. Our study was intended to assess whether it is theoretically possible to obtain self-replicating RNA polymer sequences starting from a mixture of the four monomer nucleotide bases. This is the most complex application we have so far analysed: as well as spontaneous polymerisation from four different monomers (A, C, G, U), chain growth is catalysed by longer chains with similar sequences of monomers, and there is a general fragmentation term due to hydrolysis which splits long chains into two short chains. Despite this complexity we are still able to apply the coarse-graining reduction to factor out some of the size-dependence and analyse the instabilities in the growth mechanisms which allowed some species of chain to dominate at the expense of others. We denote a chain by C_r^γ where r represents the length of the chain and γ the sequence of nucleotide bases; ψ is used to refer to an arbitrary monomer, and $\theta*$ represents the Watson-Crick complement of the chain θ. The mechanisms we include in our model are:

(i) basic chain growth: $C_r^\gamma + C_1^\psi \overset{\text{slow}}{\rightleftharpoons} C_{r+1}^{\gamma+\psi}$ — a Becker-Döring process,

(ii) template-based chain synthesis: $C_r^\gamma + C_1^\psi + C_s^\theta \overset{\text{fast}}{\rightleftharpoons} C_{r+1}^{\gamma+\psi} + C_s^\theta$, which is again a Becker-Döring process. We expect this to operate at some general rate for all chains, with the exception of when the sequence $\gamma + \psi$ is a subset of Watson-Crick complement of θ, then the process will occur at some much larger rate.

(iii) hydrolysis; here, a long chain splits into two shorter chains, corresponding to the reaction $C_{r+s}^{\gamma+\theta} \to C_r^\gamma + C_s^\theta$. Although this destroys longer chains, replacing them with shorter chains, it increases the *number* of chains, each of which have a catalytic effect on the growth of chains; thus it is not immediately clear whether this has a positive or negative role in polymerisation.

(iv) enzymatic replication, also known as replicase ribozymal activity, which we model by $C_r^\gamma + C_1^\psi + C_{r+k}^{\gamma*+\theta*} + C_s^\xi \rightleftharpoons C_{r+1}^{\gamma,\psi} + C_{r+k}^{\gamma*+\theta*} + C_s^\xi$. Here, a third chain ($C_s^\xi$) aids the growth of a chain (C_r^γ) which is already in close contact with another chain acting as a template ($C_{r+k}^{\gamma*+\theta*}$)

An analysis of the stability of the uniform solution, in which the concentrations of all chain sequences grow at the same rate, shows that such a solution is unstable for certain parameter regimes. Thus such a solution would not be observed in experiments. Instead a 'patterned' solution in which some sequences proliferate while others remain at low concentrations will be observed. Such an analysis can only be performed following a coarse-grained approximation of the full microscopic system to a reduced mesoscopic model. Thus there is a spontaneous symmetry-breaking of the large and complex polymerising nucleotide system into a number of sequence types which compete for the available resources (nucleotide monomers). This is a similar behaviour to that observed in chiral polymerisation: nonlinear feedback coupled with competition causes symmetry-breaking. The central conclusion from our study is that, assuming plausible values for prebiotic nucleotide concentrations and rate coefficients, sequence selection of self-replicating RNA polymers can indeed arise over time intervals of months to years.

6 Conclusions

Our coarse-graining approach helps to bridge the length and time scales between generalised microscopic models formulated using Becker-Döring-style theories of nucleation and growth processes. The resulting kinetic equations give rise to quantities which are observed in experimental studies and so can be tested against experimental data. A further benefit of the coarse-graining procedure which permits direct comparison with experimental results is that the resulting macroscopic models often only contain a handful of parameters, whereas the microscopic models require hundreds or thousands of rate constants to be specified.

We have shown that such ideas can be applied to a wide range of non-equilibrium phenomena.

This is due to the properties of the Becker-Döring system of equations which underpins many nucleation and growth processes. The ability to contract this system of equations using a coarse-grained renormalisation mapping permits many new results of both mathematical and physicochemical significance to be obtained. For example, similar ideas have been used in simplifying models of competitive nucleation (Wattis, [34]), and in the reduction of two-component aggregation models to single-component models in the analysis of river networks [13].

Future work will involve more detailed analysis of multi-component systems undergoing aggregation, where the vast numbers of different cluster compositions as well as cluster sizes require us to make additional reductions in model complexity before comparisons with experimental data can be made. We also plan to explore the connections between our coarse-graining procedure and more standard asymptotic methods in the hope that this may enable us to be more specific about the accuracy and ranges of validity of such theoretical approaches to the description of complex reacting systems.

Acknowledgements

This paper is dedicated to Professor Mark Child FRS on the occasion of his retirement as Coulson Professor of Theoretical Chemistry at the University of Oxford. We are grateful to PL Luisi, A Eschenmoser, CD Bolton, and JR King for stimulating conversations and contributions over several years towards the development of many of the ideas discussed here. We acknowledge EPSRC grant GR/R94916/01 for funding some of this work.

References

[1] DJ Amit. Field theory, the renormalization group and critical phenomena, McGraw Hill, London, (1978).

[2] P Bachmann, PL Luisi, J Lang. Autocatalytic self-replicating micelles as models for prebiotic structures. *Nature*, **357**, 57–59, (1992).

[3] JM Ball, J Carr. The discrete coagulation-fragmentation equations: existence, uniqueness and density conservation. *J Stat Phys*, **61**, 203–234, (1990).

[4] R Becker, W Döring. Kinetische Behandung der Keimbildung in übersättigten Dämpfen, Ann Phys **24**, 719–752, (1935).

[5] N Berclaz, E Blöchliger, M Müler, PL Luisi. Matrix effect of vesicle formation as investigated by cryotransmission electron microscopy. *J. Phys. Chem. B* **105**, 1065–1071, (2001).

[6] N Berclaz, M Müller, P Walde, P L Luisi. Growth and transformation of vesicles studied by ferritin labelling and cryotransmission electron microscopy. *J. Phys. Chem. B* **105**, 1056–1064, (2001).

[7] CM Bender, SA Orszag. Advanced Mathematical Methods for Scientists and Engineers. McGrw-Hill, Singapore, (1978).

[8] E Blöchliger, M Blocher, P Walde, PL Luisi. Matrix effect in the size distribution of fatty acid vesicles. *J. Phys. Chem. B* **102**, 10383–10390, (1998)

[9] CD Bolton, JAD Wattis. Generalised coarse-grained Becker-Döring equations. *J Phys A Math Gen*, **36**, 7859–7888, (2003).

[10] CD Bolton, JAD Wattis. The size-templating matrix effect in vesicle formation I: a microscopic model and analysis. *J Phys Chem B*, **107**, 7126–7134 (2003). CD Bolton, JAD Wattis. The size-templating matrix effect in vesicle formation II: a macroscopic model and analysis. *J Phys Chem B*, **107**, 14306–14318, (2003).

[11] J Cardy. Scaling and renormalisation in statistical physics. CUP, Cambridge, (1996).

[12] J Carr. Applications of Center Manifold Theory. Springer, New York, (1981).

[13] FP da Costa, M Grinfeld, JAD Wattis. A hierarchical cluster system based on Horton-Strahler rules for river networks. *Studies in Applied Mathematics*, **109**, 163–204, (2002).

[14] S Colonna, G Fleischaker, PL Luisi (eds). Self-production of Supramolecular Structures: from Synthetic Structures to Models of Minimal Living Systems, NATO ASI Series. Kluwer, Dordrecht, (1994).

[15] PV Coveney, RR Highfield. The Arrow of Time. Flamingo, (1991), WH Allen (1990).

[16] PV Coveney, RR Highfield. Frontiers of Complexity, Faber & Faber, (1995 &1996).

[17] PV Coveney, JAD Wattis. Analysis of a generalised Becker-Döring model of self-reproducing micelles. *Proc. Roy. Soc. Lond. A*, **452**, 2079–2102, (1996).

[18] PV Coveney, JAD Wattis. A Becker-Döring model of self-reproducing vesicles. *J. Chem. Soc.: Faraday Transactions*, **102**, 233–246, (1998).

[19] PV Coveney, JAD Wattis. Cluster renormalization for the Becker-Döring equations. *J Phys A: Math Gen*, **32**, 7145–7152, (1999).

[20] U Frisch, Turbulence: The Legacy of AN Kolmogorov. CUP, Cambridge, (1995).

[21] RF Gesteland, TR Cech, JF Atkins (eds), The RNA World, Second Edition, Cold Spring Harbour Laboratory Press, New York, (1999).

[22] N Goldenfeld. Lectures on Phase Transitions and the Renormalisation Group. Frontiers in Physics vol 85, Addison-Wesley, (1992).

[23] P Gray, SK Scott, Chemical Oscillations and Instabilities: Nonlinear Chemical Kinetics, OUP, Oxford, (1994).

[24] L Glass, MC Mackey. From Clocks to Chaos, Princeton University Press, Princeton, (1988).

[25] AL Hodgkin, AF Huxley. A quantitative description of membrane current and its application to conduction and excitation in nerve. *J Physiol (London)*, **117**, 500–544, (1952).

[26] JD Murray. Mathematical Biology, 2nd ed, Springer-Verlag, (1993).

[27] PGH Sandars. A toy model for the generation of homochirality during polymerisation. *Origins of Life and the Evolution of Biospheres*, **33**, 575–587, (2003).

[28] J Skår, PV Coveney (eds), Self-organisation, *Phil. Trans. R. Soc. Lond. A*, **361** (2003).

[29] M von Smoluchowski. Drei Vorträge über Diffusion, Brownsche Molekular Bewegung und Koagulation von Kolloidteichen. *Physik Z*, **17**, 557, (1916).

[30] P Walde, R Wick, M Fresta, A Mangone, PL Luisi. Autopoietic Self-Reproduction of Fatty Acid Vesicles. *J Am Chem Soc*, **116**, 11649–11654, (1994).

[31] JAD Wattis, PV Coveney. Generalised nucleation theory with inhibition for chemically reacting systems. *J Chem Phys*, **106**, 9122–9140, (1997).

[32] JAD Wattis, PV Coveney. Mesoscopic models of nucleation and growth processes: a challenge to experiment. *PCCP*, **1**, 2163–2176, (1999).

[33] JAD Wattis, PV Coveney. The origin of the RNA world: a kinetic model. *J Phys Chem B*, **103**, 4231–4250, (1999).

[34] JAD Wattis. A Becker-Döring model of competitive nucleation. *J Phys A: Math Gen*, **32**, 8755–8784, (1999).

[35] JAD Wattis. Similarity solutions for the Becker-Döring equations with continuous input of monomer. *J Phys A: Math Gen*, **37**, 7823–7841, (2004).

[36] JAD Wattis, PV Coveney. Renormalization-theoretic analysis of non-equilibrium phase transitions I: the Becker-Döring equations with power law rate coefficients. *J Phys A: Math Gen*, **34**, 8679–8695, (2001).

[37] JAD Wattis, PV Coveney. Renormalization-theoretic analysis of non-equilibrium phase transitions II: the effect of perturbations on rate coefficients in the Becker-Döring equations. *J Phys A: Math Gen*, **34**, 8697–8726, (2001).

[38] JAD Wattis, PV Coveney. Symmetry-breaking in chiral polymerisation. To appear in *Origins of Life and the Evolution of the Biosphere*, **35**, -, (2005). `http://arXiv.org/abs/physics/0402091`

[39] JAD Wattis, PV Coveney. Chiral polymerisation and the RNA world. *to appear in International J Astrobiology.* (2005).

[40] JAD Wattis, JR King. Asymptotic solutions of the Becker-Döring equations. *J Phys A: Math Gen*, **31**, 7169–7189, (1998).

[41] KG Wilson. Renormalization group and critical phenomena I. Renormalization group and the Kadanoff scaling picture. *Phys Rev B*, **4**, 3174–3183, (1971);

[42] KG Wilson. Renormalization group and critical phenomena II. Phase-space cell analysis of critical behavior. *Phys Rev B*, **4**, 3184–3205, (1971);

[43] KG Wilson, J Kogut. The renormalization group and the ϵ expansion. *Phys Rep C*, **12**, 75, (1974);

[44] SL Woodruff. The use of an invariance condition in the solution of multiple-scale singular perturbation problems: ordinary differential equations. *Studies in Applied Mathematics*, **90**, 225–248, (1993).

[45] SL Woodruff. A uniformly valid asymptotic solution to a matrix system of ordinary differential equations and a proof of its validity. *Studies in Applied Mathematics*, **94**, 393–413, (1995).

[46] SL Woodruff. Multiple-scale perturbation analysis of the direct interaction approximation for inertial-range turbulence. *Phys Rev E*, **52**, 3245–3248, (1995).

[47] SL Woodruff & AF Messiter. A perturbation analysis of an interaction between long and short surface waves. *Studies in Applied Mathematics*, **92**, 159-189, (1994).